THE JOURNAL OF BIOLOGICAL CHEMISTRY VOL. 289, NO. 35, pp. 24452–24462, August 29, 2014

Amine Oxidase Copper-containing 1 (*AOC1*) Is a Downstream Target Gene of the Wilms Tumor Protein, WT1, during Kidney Development*

Received for publication, March 10, 2014, and in revised form, July 9, 2014 Published, JBC Papers in Press, July 17, 2014, DOI 10.1074/jbc.M114.564336

Karin M. Kirschner, Julian F.W. Braun, Charlotte L. Jacobi, Lucas J. Rudigier, Anja Bondke Persson, and Holger Scholz[1]

From the Institut für Vegetative Physiologie, Charité-Universitätsmedizin Berlin, Charitéplatz 1, 10117 Berlin, Germany

Background: Polyamines and their diamine precursor putrescine are ubiquitous organic polycations involved in cell growth and proliferation.
Results: The Wilms tumor suppressor, WT1, stimulates transcription of the *AOC1* gene, which encodes the key enzyme for putrescine breakdown.
Conclusion: WT1-dependent regulation of putrescine degradation, mediated by AOC1, has a role in kidney morphogenesis.
Significance: The findings provide novel insights into transcriptional mechanisms controlling genitourinary development.

Amine oxidase copper-containing 1 (AOC1; formerly known as amiloride-binding protein 1) is a secreted glycoprotein that catalyzes the degradation of putrescine and histamine. Polyamines and their diamine precursor putrescine are ubiquitous to all organisms and fulfill pivotal functions in cell growth and proliferation. Despite the importance of AOC1 in regulating polyamine breakdown, very little is known about the molecular mechanisms that control its expression. We report here that the Wilms tumor protein, WT1, which is necessary for normal kidney development, activates transcription of the *AOC1* gene. Expression of a firefly luciferase reporter under control of the proximal *AOC1* promoter was significantly enhanced by co-transfection of a WT1 expression construct. Binding of WT1 protein to a *cis*-regulatory element in the *AOC1* promoter was confirmed by electrophoretic mobility shift assay and chromatin immunoprecipitation. Antisense inhibition of WT1 protein translation strongly reduced *Aoc1* transcripts in cultured murine embryonic kidneys and gonads. *Aoc1* mRNA levels correlated with WT1 protein in several cell lines. Double immunofluorescent staining revealed a co-expression of WT1 and AOC1 proteins in the developing genitourinary system of mice and rats. Strikingly, induced changes in polyamine homeostasis affected branching morphogenesis of cultured murine embryonic kidneys in a developmental stage-specific manner. These findings suggest that WT1-dependent control of polyamine breakdown, which is mediated by changes in AOC1 expression, has a role in kidney organogenesis.

Polyamines are low molecular weight organic polycations that are found in the cells of all living organisms (1). Due to their positive charges, polyamines can bind to macromolecules such as RNA, DNA, and proteins (2, 3). The natural polyamines spermidine and spermine and their diamine precursor putrescine regulate a variety of physiological processes including gene expression, membrane stabilization, ion channel gating, and cell proliferation (1, 4). Polyamines have been implicated in various pathologies, *e.g.* stroke, tumor expansion, inflammation, and ischemic tissue injury (5–9). Consistent with their roles in cell growth and survival, high amounts of polyamines have been detected in proliferating cells during development but also in mature tissues with extensive protein synthesis (1).

The rate-limiting step in polyamine biosynthesis is the conversion of the amino acid ornithine to the diamine precursor putrescine, which is catalyzed by ornithine decarboxylase 1 (ODC1).[2] Addition of two aminopropyl groups to putrescine in a two-step reaction produces spermidine and spermine, respectively (10, 11). Recent findings indicate that the availability of polyamines is determined not only by the rate of synthesis but also by the activity of the degradation pathways. Although spermine and spermidine are degraded by the consecutive action of spermidine/spermine N^1-acetyltransferase 1 and polyamine oxidase, putrescine is the preferred substrate for breakdown by amine oxidase copper-containing 1 (AOC1; formerly known as amiloride-binding protein 1) (12, 13).

AOC1 is a homodimeric glycoprotein with an apparent molecular mass of 186 kDa that was initially thought to constitute a component of the amiloride-sensitive sodium channel (14, 15). Subsequent studies revealed that AOC1 is indeed a secreted diamine oxidase, which deaminates putrescine and histamine, thereby generating hydrogen peroxide (16, 17). Enzymatic activity of AOC1 can be inhibited by amiloride and some of its derivatives such as aminoguanidine (18, 19). AOC1 is strongly expressed in the kidneys (20, 21), placenta (22), intestine (23, 24), and lungs with lower levels in the brain (21, 25). Very little is known about the molecular mechanisms regulating *AOC1* gene expression. The proximal *AOC1* promoter

* This work was supported by Deutsche Forschungsgemeinschaft Grant Scho634/8-1.
[1] To whom correspondence should be addressed: Inst. für Vegetative Physiologie, Charité-Universitätsmedizin Berlin, Charitéplatz 1, 10117 Berlin, Germany. Tel.: 49-30-450-528213; Fax: 49-30-450-528928; E-mail: holger.scholz@charite.de.

[2] The abbreviations used are: ODC1, ornithine decarboxylase 1; AOC1, amine oxidase copper-containing 1; d.p.c., day(s) postconception.

region is GC-rich and displays no TATA box, CAAT box, or consensus initiator sequence (16). Liang *et al.* (26) reported that estrogen can induce *AOC1* expression via CCAAT/enhancer-binding protein-β in mouse uterus during embryo implantation and decidualization. Other putative *trans*-acting factors include cyclic AMP, bone morphogenetic protein 2, and ERK1/2 (26).

Recent findings indicate that polyamines are involved in normal kidney development (27). Nephrogenesis is accomplished by the reciprocal interaction between two tissues: the epithelial ureteric bud, which is formed from the nephric duct, and the surrounding metanephric mesenchyme (28). Signals derived from the metanephric blastema stimulate the dichotomous branching of the invading ureteric bud, which in turn induces the mesenchymal cells to condense, aggregate, and undergo nephron differentiation (28). Hence, kidney morphogenesis relies on a mesenchymal-to-epithelial transition that is regulated by various transcription factors and secreted molecules.

Interestingly, ODC1 inhibition in *ex vivo* cultured murine embryonic kidneys resulted in a smaller organ size, fewer epithelial ureteric bud branches, and delayed tubule formation (27). These dysmorphologies were associated with reduced cell proliferation and alteration in mesenchymal gene expression, suggesting that polyamines are important for normal murine kidney development (27). *ODC1* expression is controlled on the molecular level by the transcription factor WT1, which can either repress or activate the proximal *ODC1* promoter depending on the cellular context (29). Mice with homozygous *Wt1* deletion ($Wt1^{-/-}$) are embryonic lethal and exhibit agenesis of the kidneys and gonads among other defects (30–35). Thus, regulation of polyamine synthesis appears to be one of the mechanisms by which WT1 facilitates the formation of the genitourinary system. However, the exact role of WT1 in regulating polyamine homeostasis, in particular its degradation pathway, has not been explored yet. In view of this background, our study served a 2-fold purpose. First, it was aimed at analyzing the distribution of AOC1 in developing kidneys. Second, we examined whether expression of the gene encoding AOC1 is regulated by the Wilms tumor transcription factor, WT1. We report here that *AOC1* is indeed a transcriptional downstream target gene of WT1. Importantly, AOC1 inhibition influenced branching morphogenesis of cultured murine embryonic kidneys in a developmental stage-dependent manner. These results suggest a role for AOC1 in the formation of the murine genitourinary system.

EXPERIMENTAL PROCEDURES

Animals—Mouse breeding pairs (C57/BL6 strain) were mated in the in-house animal facility in compliance with the local laws (permit number T0308/12). The morning of vaginal plugs was considered as 0.5 day postconception (d.p.c.). Sex determination of the embryos was performed by PCR amplification of the Y chromosomal gene *Kdm5d* from genomic DNA using the following primers: mKdm5d-F, CTGAAGCTTTTGGCTTTGAG; mKdm5d-R, CCACTGCCAAATTCTTTGG (36).

Cell Culture—Human embryonic kidney (HEK) 293 cells (catalogue number ACC 305) were obtained from the German Collection of Microorganisms and Cell Cultures (DSMZ, Braunschweig, Germany) and kept in DMEM/nutrient mixture (PAA Laboratories, Pasching, Austria) supplemented with 10% FCS (Biochrom KG, Berlin, Germany) and L-glutamine (PAA Laboratories). The human osteosarcoma-derived UB27 and UD28 cell lines, which contain the murine WT1(−KTS) and WT1(+KTS) protein isoforms, respectively, regulated through a tetracycline-dependent promoter, were gifts from Dr. Christoph Englert. UB27 and UD28 cells and the murine mesonephros-derived M15 cell line were cultured as described elsewhere (37–39).

TABLE 1
PCR primers
qPCR, quantitative PCR.

Primer	Sequence
Cloning primers	
hAOC1-Prom-301	GTCGGTACCCTGTCAGCTTCAGGTAAG
hAOC1-Prom-47	ATTGGTACCTCCTAGGCCAGCTCAGGC
hAOC1-Prom-R	GCAGCTAGCCCCAGTTCGCTCTGCTTC
hAOC1-Prom Mut-F	GTCACTTACTGCATTGCATG
hAOC1-Prom Mut-R	CATGCAATGCAGTAAGTGAC
qPCR Primers	
hAOC1-F	CGGCCTTCCGCTTCAAAA
hAOC1-R	TGCTCAAAGACCACGGGC
mAOC1-F	GGAACAAAGTCTGGGAGC
mAOC1-R	GGCCAAAGTCAGATTCTTG
mOdc1-F	CCTCAGTGTTAAGTTTGGTGC
mOdc1-R	CACTGGTGATCTCTTCAAATT
hGAPDH-F	ACAGTCAGCCGCATCTTCTT
hGAPDH-R	GACAAGCTTCCCGTTCTCAG
mGapdh-F	ACGACCCCTTCATTGACCTCA
mGapdh-R	TTTGGCTCCACCCTTCAAGTG
ChIP primers	
mAoc1-ChIP-F	ACACAGTATGTAACAGAGAAAGCCA
mAoc1-ChIP-R	CCACTGACACAAGAAGTCTTCTTAA
mActin-ChIP-F	ATAGGACTCCCTTCTATGAGC
mActin-ChIP-R	TCCACTTAGACCTACTGTGCA
mAmhr2-PromBS-F	CAGCTGGACAGCCAAGGTC
mAmhr2-PromBS-R	CAGCCAAGGCTTCCTACAAA

Plasmids—A 367-base pair (bp) DNA sequence (from −301 to +66 bp relative to the transcription start site) and a 113-bp DNA sequence (from −47 to +66 bp relative to the transcription start site) of the human *AOC1* gene (Ensembl accession number ENSG00000002726) were cloned by PCR utilizing a bacterial artificial chromosome (imaGenes, Berlin, Germany, clone RP4-548K24) as template. The amplified product was ligated into the KpnI and NheI restriction sites of the pGL3-Basic reporter plasmid (Promega, Mannheim, Germany). The PCR primers that were used for DNA amplification are listed in Table 1. Site-directed base pair mutations were introduced in the *AOC1* promoter sequence by PCR as described elsewhere (40, 41). All constructs were analyzed by automated DNA sequencing (EurofinsMWG, Ebersberg, Germany). The expression construct for the murine WT1(−KTS) protein was kindly provided by Dr. Daniel Haber (Massachusetts General Hospital, Boston, MA).

Cell Transfections and Reporter Gene Assays—HEK293 cells were expanded to ~40% confluence in 24-well tissue culture plates. Firefly luciferase constructs (150 ng each) harboring the indicated sequences of the human *AOC1* promoter were transiently transfected along with a WT1(−KTS) expression construct (150 ng) and a *Renilla* luciferase plasmid (50 ng) using the FuGENE 6® reagent (1 μl/well) as described in the supplier's manual (Promega). As negative controls, transfections were

TABLE 2
Oligonucleotides used for gel shift experiments (mutated nucleotides are underlined)

Oligonucleotide	Sequence
hAOC1-WT1-sense	GTCCCTCCCTGCAGGGCGGGGTCTG
hAOC1-WT1-antisense	CAGACCCCGCCCTGCAGGGAGGGAC
hAOC1-WT1mut-sense	GTCACTTACTGCATTGCATGGTCTG
hAOC1-WT1mut-antisense	CAGACC[underln]ATGCAATGCAGTAAGTGAC
mAdamts16-wtA-sense	TCCTCTATCCCCTCCCCTCTCCTCTCCTTT
mAdamts16-wtA-antisense	AAAGGAGAGGAGAGGGGAGGGGATAGAGGA

performed with the pGL3-Basic reporter plasmid (Promega) and the empty pCB6+ expression vector, respectively. After 24 h, the transfected cells were lysed in Reporter Lysis Buffer (Promega), and luciferase activities were measured in a luminometer (FB 12 luminometer, Berthold Detection Systems, Pforzheim, Germany) as described (40, 41). Data are presented as the ratios of firefly *versus Renilla* luciferase activities.

Transfection of siRNA—M15 cells were grown to ~60% confluence in 6-well culture plates. A pool of four different siRNAs (50 pmol/well; Dharmacon, Thermo Fisher Scientific) targeting the murine *Wt1* gene (ON-TARGETplus, SMARTpool siRNA, L-040686-01-0005; NCBI Reference Sequence NM_144783) were transfected with DharmaFECT 1 reagent (Dharmacon) (39). Four different non-targeting siRNAs (siGENOME non-targeting siRNA pool 2, Dharmacon) were used as a negative control. The cells were harvested for mRNA and protein analysis 48 h after siRNA transfection.

Electrophoretic Mobility Shift Assay (EMSA)—Non-radioactive EMSAs were performed with purified GST-tagged recombinant WT1 protein (42) and double-stranded oligonucleotides (Table 2), which were selected on the basis of predicted WT1 binding sites in the proximal promoter of the human *AOC1* gene. All oligonucleotides were 3′-digoxigenin-labeled using the DIG Oligonucleotide 3′-End Labeling kit (Roche Applied Science). Likewise, double-stranded oligonucleotides with mutations in the WT1 binding motifs (Table 2) were 3′-digoxigenin-labeled. For competition experiments, we used an oligonucleotide with a previously identified WT1 binding sequence in the promoter of the murine *Adamts16* gene (43). The binding reactions were carried out at room temperature for 1 h using 0.75 μg of recombinant WT1 protein and 1 pmol of labeled oligonucleotide in 1× reaction buffer (10 mM Tris-HCl, pH 7.5, 50 mM KCl, 50 mM NaCl, 1 mM $MgCl_2$, 1 mM EDTA, 5 mM DTT, 5 mM phenylmethylsulfonyl fluoride). DNA-bound proteins were separated on a non-denaturing 6% polyacrylamide gel and transferred with a semidry blotting system (Bio-Rad) on a positively charged nylon membrane (Roche Applied Science). After UV cross-linking (Stratalinker® UV cross-linker, Stratagene) and treatment with blocking reagent (Roche Applied Science), the membrane was incubated with anti-3′-digoxigenin-alkaline phosphatase antibody (diluted 1:10,000; catalogue number 11093274910, Roche Applied Science). Proteins were detected by nitro blue tetrazolium/5-bromo-4-chloro-3-indolyl phosphate staining (Roche Applied Science).

Chromatin Immunoprecipitation (ChIP) Assay—M15 cells were expanded in 10-cm tissue culture plates to ~80% confluence and used at ~1×10^6 cells per assay. After fixation with 4% formaldehyde, the cells were disrupted by ultrasonication (Labsonic U, B. Braun, Melsungen, Germany) and centrifuged. The supernatants were diluted in immunoprecipitation buffer (0.01% SDS, 1.1% Triton X-100, 1.2 mM EDTA, 16.7 mM Tris-HCl, pH 8.1) and precleared for 1 h at 4 °C with DNA-blocked protein G-agarose (Merck Millipore). The following antibodies and control sera were used (0.6 μg each) for overnight incubation at 4 °C: normal rabbit IgG (catalogue number sc-2027, Santa Cruz Biotechnology, Inc., Santa Cruz, CA), rabbit polyclonal anti-WT1 antibody (catalogue number sc-192, Santa Cruz Biotechnology, Inc.). The immunoprecipitates were bound to DNA-blocked protein G-agarose during 1-h incubation at 4 °C. Following several washing steps, the DNA was eluted in 1% SDS, 0.1 M $NaHCO_3$; extracted in 25:24:1 phenol/chloroform/isoamyl alcohol according to the supplier's instructions (Invitrogen); and subsequently precipitated in 100% ethanol. Immunoprecipitated DNA was amplified by quantitative PCR using primer pairs that flanked the identified WT1 binding sites in the murine *Aoc1* promoter and normalized to DNA amplified from the last intron of the murine β-actin gene.

Organ Culture Experiments—Kidneys and gonads were excised from embryos of timed pregnant mice (C57BL6 strain). The matched organs of each embryo were cultured separately on two polyethylene terephthalate Transwell® filters with 0.4-μm pore size (Corning, Inc.). This procedure allowed for a pairwise comparison between cultured explants from a single donor. The Transwell filters were kept in DMEM/nutrient mixture with stable L-glutamine supplemented with 10% FCS, 100 IU/ml penicillin (PAA Laboratories), and 100 μg/ml streptomycin (PAA Laboratories) at 37 °C in a humidified atmosphere with 5% CO_2. To study branching morphogenesis, the kidneys were isolated from mouse embryos at the indicated developmental stages and cultured *ex vivo* as described elsewhere (43). The organ rudiments were treated with 1 μg/μl AOC1 protein isolated from pig kidneys (Sigma-Aldrich), 100 μM putrescine (Sigma-Aldrich), or 1 μM AOC1 inhibitor aminoguanidine (Sigma-Aldrich). In some experiments, 200 μM L-ascorbic acid (vitamin C; Roth, Karlsruhe, Germany) was added to the culture medium of the preparations. After 72 h, the explants were formalin-fixed and double stained with FITC-conjugated anti-pancytokeratin antibody (diluted 1:100; Sigma-Aldrich). Photographs were taken, and branching of the pancytokeratin-stained ureter was analyzed using ImageJ software (National Institutes of Health, Bethesda, MD). Knockdown of WT1 was achieved by incubation of the organ cultures for 72 h either with *Wt1* antisense (CAGGTCCCGCACGTCGGAACCCAT) or mismatch (CAGCTCCGGCACCTCGCAACCGATG) *vivo*-morpholinos at 10 μM each (Gene Tools, Philomath, OR) (44). Whole cell lysates and total RNA were prepared from cultured organs and cells as described below.

Preparation of RNA and Reverse Transcription (RT)-Quantitative PCR—Total RNA was isolated from tissues and primary cells with the RNeasy Micro kit (Qiagen, Hilden, Germany) and from permanent cell lines with the TRIzol LS reagent (Invitrogen). First strand cDNA synthesis was carried out using oligo-(dT) primers and Superscript™ II reverse transcriptase (Invitrogen). Real time PCR amplification was performed with SYBR® Green PCR Master Mix and the StepOnePlus™ system (Invitrogen) as described in detail elsewhere (45). The PCR primers for real time RT-PCR are listed in Table 1. Relative transcript levels were obtained by subtracting the threshold cycle (Ct) value of the housekeeping gene (β-actin or *Gapdh*) from the corresponding threshold cycle value of the gene of interest. Differences in mRNA levels were calculated according to the expression $2^{\Delta\Delta Ct}$.

Immunohistochemistry—Immunofluorescent stainings were performed on mouse and rat tissues as described in detail elsewhere (40, 41). Briefly, mouse (13.5 d.p.c.) and rat embryos (16.5 d.p.c.) were fixed in 4% formaldehyde overnight, frozen in tissue-Tek O.C.T. compound (Sakura Finetek, Zoeterwoude, Netherlands), and sectioned on a cryostat. Frozen sections (8 μm) were thawed and cooked in citrate buffer (18 mM citric acid, 82 mM trisodium citrate, 0.05% (v/v) Tween 20, pH 6.0) for 7 s in a microwave oven and subsequently blocked for 5 min at room temperature in serum-free DakoCytomation protein block (catalogue number X0909, Dako, Hamburg, Germany). Single immunostainings for WT1 and AOC1 were performed on mouse tissues using the following primary antibodies diluted in ready-to-use antibody diluent (Zymed Laboratories Inc.): rabbit polyclonal anti-AOC1 (diluted 1:300; catalogue number AV41908, Sigma-Aldrich), rabbit polyclonal anti-WT1 (diluted 1:75; catalogue number sc-846, Santa Cruz Biotechnology, Inc.). Double immunostainings were performed on rat tissues using the above anti-AOC1 antibody in combination with the anti-WT1 monoclonal mouse F6 antibody (diluted 1:600; catalogue number MAB4234, Millipore). For visualization of the bound primary antibodies, Cy3-AffiniPure donkey anti-rabbit IgG (diluted 1:200; catalogue number 711-165-152, Jackson ImmunoResearch Laboratories) and Alexa Fluor® 488-AffiniPure donkey anti-mouse IgG (diluted 1:100; catalogue number 715-545-151, Jackson ImmunoResearch Laboratories) were used. The cell nuclei were counterstained with 4′,6-diamidino-2-phenylindole (DAPI). Pictures of double stainings were taken with a digital camera connected to a confocal microscope (Leica DM 2500, Leica Microsystems, Wetzlar, Germany) utilizing LAS AF Lite software (Leica Microsystems). An epifluorescence microscope (Axiovert100, Carl Zeiss, Berlin, Germany) connected to a digital camera (Spot RT Slider, Diagnostic Instruments, Sterling Heights, MI) with Spot software (Universal Imaging Corp., Marlow Buckinghamshire, UK) was used for pictures of single stainings.

SDS-PAGE and Immunoblotting—Cells and tissues were lysed in Laemmli buffer (50 mM Tris-HCl, pH 6.8, 4 M urea, 1% (w/v) SDS, 7.5 mM DTT), disrupted by ultrasonication (Labsonic U), and subsequently heated to 95 °C for 5 min. Protein concentrations were measured spectrophotometrically. Bromphenol blue (0.001%, w/v) was added, and 20 μg of protein were loaded per lane and separated on a 10% denaturing polyacrylamide gel. The proteins were transferred onto a polyvinylidene difluoride membrane (GE Healthcare) with the use of a semidry blotting apparatus (Bio-Rad). Nonspecific binding activity was reduced by incubating the membranes for 60 min at room temperature in 5% nonfat milk (Roth) in TBS, 0.1% Tween 20. Incubation with WT1 antibody (diluted 1:400; C19, catalogue number sc-192, Santa Cruz Biotechnology, Inc.) in 2.5% nonfat milk (Roth) in TBS/Tween 20 was performed overnight at 4 °C. After washing with TBS/Tween 20, the antibodies were detected with a peroxidase-coupled IgG (diluted 1:20,000; donkey anti-rabbit IgG-HRP, catalogue number sc-2313, Santa Cruz Biotechnology, Inc.), and the reaction products were visualized with Western Lightning™ Plus ECL reagents (PerkinElmer Life Sciences) following the user's manual. Equal protein loading was assessed with an actin antibody (diluted 1:6,000; anti-actin clone C4, catalogue number MAB1501R, Millipore) after stripping the membranes with 1:5 diluted 1 N NaOH in distilled water for 10 min.

Statistics—Two-tailed Student's *t* test (paired and unpaired) and analysis of variance with Tukey's post hoc test were performed as indicated to reveal statistical significances. *p* values less than 0.05 were considered significant.

RESULTS

AOC1 and WT1 Proteins Are Co-expressed in Embryonic Kidneys—Although AOC1 protein can be isolated from the kidneys of various species (20, 21), little is known about its cellular localization and function during embryonic development. We used a polyclonal rabbit anti-AOC1 antibody to visualize AOC1-expressing cells in developing kidneys. Anti-WT1 antibodies raised in rabbit and mouse were used to detect WT1 protein in tissue sections of mice and rats, respectively. Single immunostainings of AOC1 and WT1 on consecutive slices of mouse embryos (13.5 d.p.c.) identified both proteins in the developing kidney, testis, and mesonephros (Fig. 1, *a* and *b*). AOC1 immunoreactivity was also visible in the adrenal gland (Fig. 1*a*). No fluorescence signal was obtained when normal rabbit serum instead of primary antibodies was used (Fig. 1*c*). Double immunostainings on tissue sections of rat embryos (16.5 d.p.c.) established an overlapping distribution of AOC1 and WT1 proteins in the glomerular precursors of the developing kidney (Fig. 1, *d*–*g*). Additional AOC1 immunoreactivity was detected in renal cells, which did not contain WT1 (Fig. 1, *d*, *e*, and *g*).

Knockdown of WT1 in Embryonic Kidneys and Gonads Reduces AOC1 Expression—Co-expression of AOC1 and WT1 suggests a regulatory link between both proteins in different cell types of the genitourinary system (Fig. 1). We therefore addressed the question of whether WT1 is indeed necessary for normal expression of *Aoc1* in embryonic kidneys and gonads. To this end, WT1 protein translation was inhibited in cultured murine embryonic kidneys utilizing a sequence-specific *Wt1 vivo*-morpholino (*Wt1* morpholino) (Fig. 2). Incubation of the contralateral kidney with a *Wt1* mismatch *vivo*-morpholino (mismatch morpholino) containing five non-matching nucleotides served as a negative control. *Aoc1* mRNA expression was analyzed by RT-real time PCR after 72 h of culture in the presence of either *Wt1* or mismatch *vivo*-morpholino. Knockdown

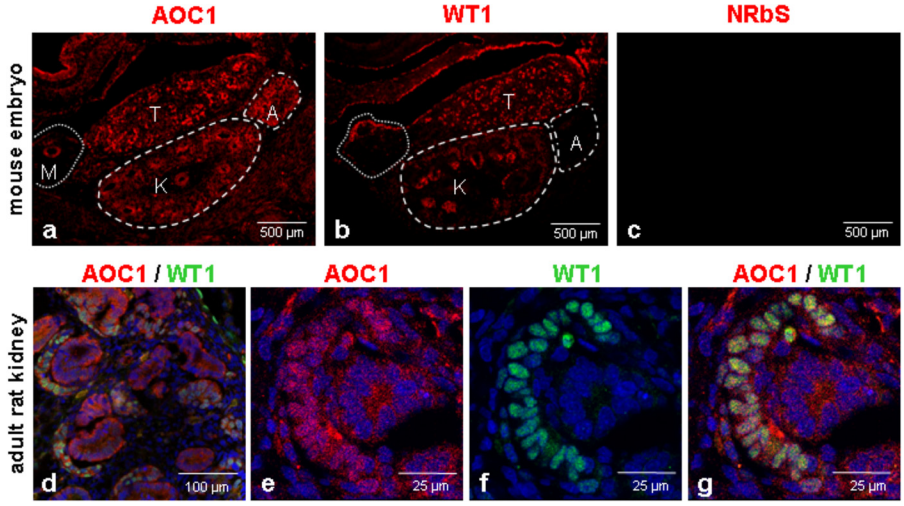

FIGURE 1. **AOC1 and WT1 protein expression in embryonic kidneys and gonads.** Serial cryosections of a mouse embryo (13.5 d.p.c.) were stained with antibodies against AOC1 (*a*) and WT1 (*b*), respectively. Normal rabbit serum (*NRbS*) was used as a negative control (*c*). *K*, kidney; *T*, testis; *M*, mesonephros; *A*, adrenal gland. Representative double immunolabeling of AOC1 and WT1 in a 16.5 d.p.c. embryonic rat kidney (*d–g*) is shown. AOC1 (*red*) and WT1 (*green*) proteins were visualized with Cy3- and Alexa Fluor 488-conjugated secondary antibodies, respectively. Co-localization of AOC1 and WT1 in cells of the developing glomeruli is indicated by the *yellow* fluorescence signal in the merged image (*g*). Note that AOC1 protein is also present in cells that do not contain WT1 (*d* and *g*).

of WT1 significantly reduced *Aoc1* mRNA levels in the kidneys at 11.5, 12.5, and 13.5 d.p.c. by 70.8 ± 32.2, 51.9 ± 38.5, and 33.5 ± 22.5%, respectively (Fig. 2*A*). Knockdown efficiencies were assessed by immunoblotting with anti-WT1 antibody. Representative immunoblots are shown below the bar graphs (Fig. 2*C*). Interestingly, mRNA levels of *Odc1*, a known target gene of WT1 (29, 46), were reduced by 26.1 ± 37.6 (11.5 d.p.c., $n = 11$) and 30.0 ± 29.0% (12.5 d.p.c., $n = 12$) in kidneys treated with *Wt1* morpholino ($p < 0.05$, paired *t* test). No significant changes in *Odc1* transcripts were observed between *Wt1* morpholino- and mismatch morpholino-treated kidneys at 13.5 d.p.c. ($n = 6$) (Fig. 2*B*). Antisense inhibition of WT1 was associated with a significant reduction of intrarenal ureter branching at different developmental stages (Fig. 2*D*). In line with the findings made on embryonic kidneys, WT1 was required for normal *Aoc1* mRNA levels also in the developing gonads of male and female mice. Thus, WT1 knockdown reduced *Aoc1* transcripts in the testis by 72.6 ± 25.871.4 ± 21.8, and 30.3 ± 66.0% at 11.5, 12.5, and 13.5 d.p.c., respectively (Fig. 3*A*), and in the ovary by 65.3 ± 32.6 (11.5 d.p.c.), 57.0 ± 41.1 (12.5 d.p.c.), and 41.4 ± 51.8% (13.5 d.p.c.) (Fig. 3*B*). These findings indicate that WT1 is necessary for normal expression of *Aoc1* in murine embryonic kidneys and gonads, particularly during the early developmental stages.

Aoc1 mRNA Levels Correlate with WT1 Protein in Permanent Cell Lines—The murine mesonephros-derived cell line M15 was used to explore whether *Aoc1* transcript levels are affected by changes in cellular WT1 protein content. For this purpose, endogenous WT1 expression was inhibited by transfection of M15 cells with a pool of four different sequence-specific *Wt1* siRNAs. Pooled non-targeting siRNAs were transfected as controls. *Aoc1* transcripts were determined by RT-real time PCR, and knockdown efficiency was assessed by immunoblotting with anti-WT1 antibody. Silencing of *Wt1* in M15 cells significantly reduced *Aoc1* mRNA levels by 63.1 ± 28.4% ($p < 0.05$ *t* test) (Fig. 4*A*). Importantly, the primary *Wt1* transcript is subject to alternative splicing. The usage of an alternative splice donor site at the end of exon 9 leads to the insertion of three additional amino acids, lysine, threonine, and serine (KTS), between zinc fingers 3 and 4 of the WT1 protein (47). Structural and functional data demonstrate that WT1(−KTS) proteins, which lack the tripeptide, act as transcription factors (48, 49). Compared with the WT1(−KTS) isoforms, WT1 proteins with the KTS insertion exhibit increased RNA binding affinity and have a presumed role in mRNA processing (50, 51). To distinguish whether the *AOC1* gene is regulated predominantly by the WT1(−KTS) protein or by the WT1(+KTS) splice variant, we made use of cell lines with exclusive expression of either WT1 isoform. The UB27 and UD28 cell lines contain the WT1(−KTS) and the WT1(+KTS) splice variants, respectively, under the control of a tetracycline-sensitive promoter (37). Removal of tetracycline from the culture medium resulted in a comparable increase of WT1 protein in both cell lines (Fig. 4*D*). Notably, *AOC1* transcripts were elevated 3.4 ± 1.5- and 3.4 ± 1.1-fold at 48 and 72 h after induction of WT(−KTS) in UB27 cells ($F(3,10) = 8.195$, $p < 0.05$, analysis of variance) (Fig. 4*B*). However, no significant changes in *AOC1* mRNA levels were measured in response to induction of WT1(+KTS) in UD28 cells (Fig. 4*C*). These data demonstrate that *AOC1* expression is stimulated by the WT1(−KTS) protein.

The WT1(−KTS) Isoform Activates the AOC1 Promoter—To determine whether WT1(−KTS) protein stimulates the *AOC1* promoter directly, a luciferase reporter vector was cloned and co-transfected in HEK293 cells along with a WT1(−KTS) expression plasmid (Fig. 5*A*). Sequence analysis predicted a high affinity WT1 binding site in the proximal promoter of the *AOC1* gene that was conserved among human and mouse. This element was located between −21 and −1 bp relative to the transcription start site (+1) in the human *AOC1* promoter. Three different human *AOC1* promoter reporter constructs were generated. One construct, pAOC1prom-301, contained the presumed WT1 binding site in a sequence extending from

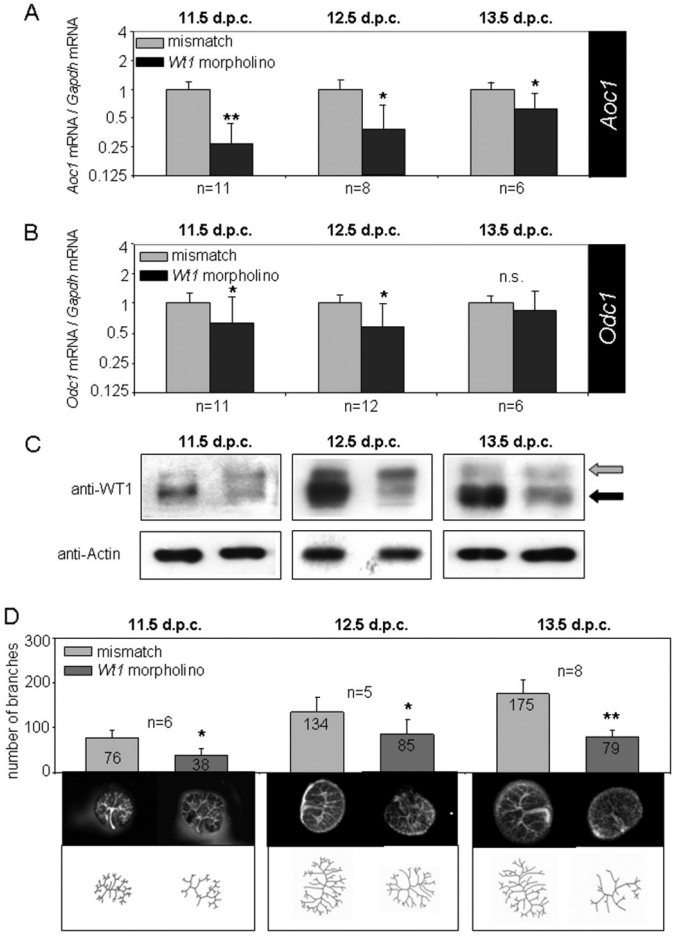

FIGURE 2. ***Aoc1* and *Odc1* mRNA in cultured murine embryonic kidneys.** Both kidneys were isolated from murine embryos at 11.5, 12.5, and 13.5 d.p.c. and cultured for 72 h in the presence of either *Wt1* antisense (*Wt1 morpholino*) or mismatch *vivo*-morpholino (*mismatch*). *Aoc1* and *Odc1* transcripts were measured by real time RT-PCR and normalized to *Gapdh* mRNA. A pairwise comparison was performed between kidneys incubated with *Wt1* morpholino and mismatch morpholino. Values of the mismatch morpholino-treated kidneys were set to 1. Significant differences in *Aoc1* (*A*) and *Odc1* (*B*) mRNA levels are indicated (*, $p < 0.05$; **, $p < 0.005$; Student's paired *t* test). Knockdown efficiencies were assessed by immunoblotting with anti-WT1 antibody using actin as a loading control (*C*). *n.s.*, not significant. *D*, analysis of ureter branching in kidneys (11.5, 12.5, and 13.5 d.p.c.) treated with either *Wt1* or mismatch *vivo*-morpholino (10 μM each). After 48 h of culture in the presence of *vivo*-morpholinos, the whole mount preparations were stained with a FITC-conjugated anti-pancytokeratin antibody (dark field images), and a skeleton of the ureter was extracted manually (schematic images). Branching of the ureter was analyzed from the schematic images. Data are presented as means ± S.D. (*error bars*). * ($p < 0.05$) and ** ($p < 0.005$) indicate significant differences (Student's paired *t* test).

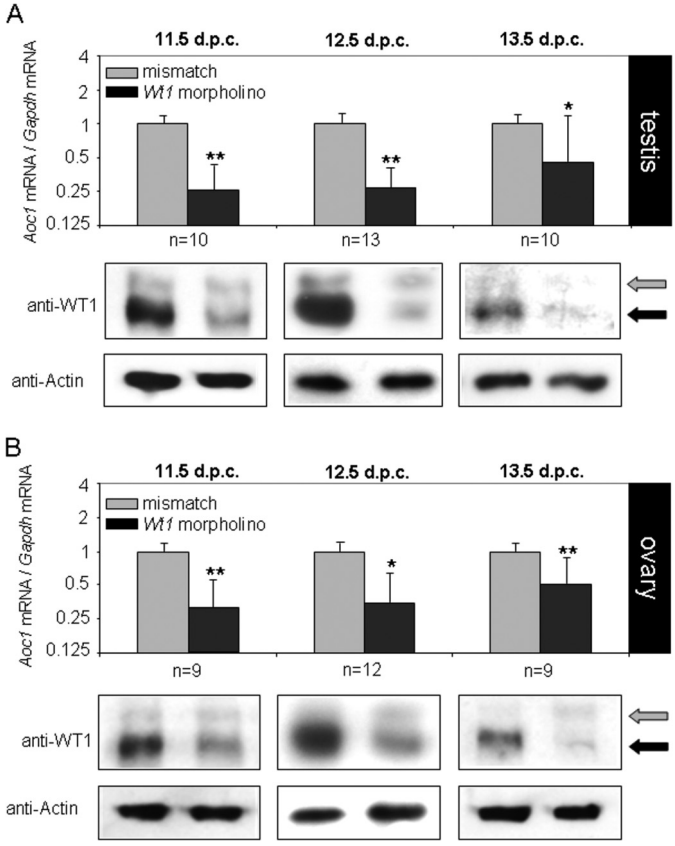

FIGURE 3. ***Aoc1* mRNA in cultured murine embryonic testis and ovary.** The gonads were isolated from male (*A*) and female (*B*) murine embryos at the indicated developmental stages and cultured for 72 h in the presence of either *Wt1* antisense (*Wt1 morpholino*) or mismatch *vivo*-morpholino (*mismatch*). *Aoc1* transcripts were quantified by real time RT-PCR and normalized to *Gapdh* mRNA. A pairwise comparison was performed between *Wt1* morpholino-treated gonads and the mismatch morpholino controls. Significant differences are indicated (*, $p < 0.05$; **, $p < 0.005$; Student's paired *t* test). Representative WT1 immunoblots to assess knockdown efficiencies are shown below the bar graphs.

−301 to +66 bp relative to the transcription start site. The second construct, pAOC1prom-47, spanned from −47 to +66 bp, and the third reporter vector, pAOC1prom-301mut, contained the 367-bp insert with a mutated WT1 binding motif. Transfection of the empty pGL3-Basic reporter plasmid served as a negative control. The two constructs, pAOC1prom-301 and pAOC1prom-47, were stimulated 2.6 ± 0.7- and 3.3 ± 1.2-fold ($p < 0.05$ *t* test), respectively, by co-transfection of the WT1(−KTS) expression vector (Fig. 5*A*). In contrast, WT1(−KTS) exerted no significant effect on pAOCp1prom-301mut in which the predicted WT1 binding site had been mutated (Fig. 5*A*). An electrophoretic mobility shift assay was performed to investigate whether WT1(−KTS) protein bound to this identified element (Fig. 5*B*). For that purpose, recombinant WT1(−KTS) protein was incubated with a digoxigenin-labeled double-stranded DNA oligonucleotide carrying the predicted WT1 binding site in the *AOC1* promoter (Fig. 5*B*, *lane 2*). Binding of WT1(−KTS) to this oligonucleotide resulted in a band shift (*arrow*) that was eliminated by addition of a non-labeled competitor (Fig. 5*B*, *lanes 3–5*). The competitor consisted of an oligonucleotide (used at a 10-, 50- and 100-fold molar excess) that contained the previously identified WT1 binding element of the murine *Adamts16* promoter (43). Binding of Wt1(−KTS) protein to the *AOC1* promoter oligonucleotide was abolished upon introducing single base pair mutations (Fig. 5*B*, *lane 7*). These results demonstrate that WT1(−KTS) protein stimulates the promoter of the *AOC1* gene by interacting with a specific *cis*-regulatory element. ChIP was carried out to explore whether WT1 protein binds to the promoter of the *Aoc1* gene in a natural chromosomal context (Fig. 5*C*). To this end, the chromatin of M15 cells was incubated either with anti-WT1 antibody or with normal rabbit serum. The amount of precipitated DNA was determined by real time PCR using specific primers for amplification of the murine *Aoc1* promoter. Compared with the use of normal rabbit serum,

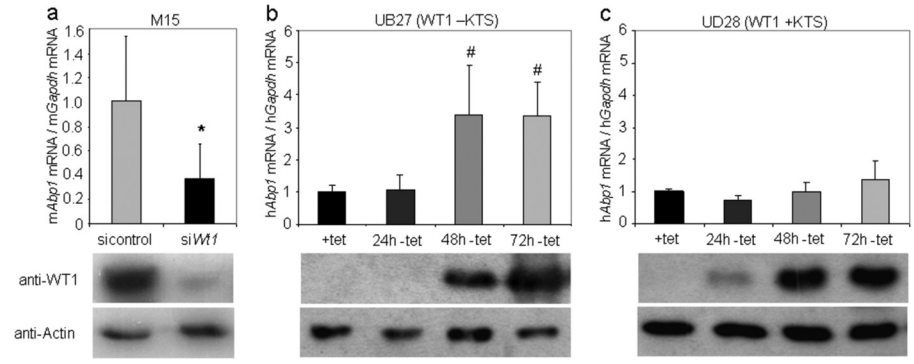

FIGURE 4. ***Aoc1* transcripts and WT1 protein in permanent cell lines.** *A*, murine mesonephros-derived M15 cells were transfected either with a pool of four different siRNAs targeting the *Wt1* gene (*siWt1*) or with non-targeting siRNAs (*sicontrol*). *Aoc1* and *Gapdh* transcripts in siRNA-transfected M15 cells were quantified by real time RT-PCR. Down-regulation of WT1 protein in response to RNA interference was assessed by immunoblot analysis using anti-WT1 antibody. Detection of actin protein served as a loading control (*D*). *B* and *C*, *Aoc1* mRNA in osteosarcoma-derived UB27 and UD28 cells, which express the WT1(−KTS) and WT1(+KTS) isoforms, respectively. *AOC1* and *GAPDH* transcripts were measured by real time RT-PCR. Temporal changes of WT1 protein in response to tetracycline depletion were detected by immunoblot analysis. Values are shown as means ± S.D. (M15 cells, $n = 5$; UB27 cells, $n = 4$; UD28 cells, $n = 3$). Statistical significance is indicated by an *asterisk* (*t* test, $p < 0.05$) or *hash tag* (analysis of variance, $F(3,10) = 8.195$, $p < 0.05$).

incubation with anti-WT1 antibody resulted in a significant increase of *Aoc1* promoter DNA (2.1 ± 1.2-fold, $p < 0.05$, *t* test). Enrichment (1.7 ± 0.7-fold, $p < 0.05$, *t* test) of the *Amhr2* promoter, a known target gene of WT1 (52), was used as a positive control.

AOC1 Affects Branching Morphogenesis in Cultured Murine Embryonic Kidneys—The potential role of AOC1 in kidney morphogenesis was studied with murine organ explants. For this purpose, the kidneys were excised from mouse embryos of stages 11.5, 12.5, and 13.5 d.p.c. and incubated *ex vivo* in the presence of AOC1 (50 milliunits/ml) from porcine kidney. For comparison, 1 unit of AOC1 catalyzes 1 μmol of putrescine in 1 h at 37 °C. Equimolar amounts of bovine serum albumin (BSA) served as a control (Fig. 6*A*). Branching of the intrarenal ureter was visualized with a FITC-conjugated anti-pancytokeratin antibody. Addition of AOC1 significantly reduced the numbers of ureter branches during the developmental stages 11.5, 12.5 and 13.5 d.p.c. by 16.4 ± 22.8, 10.2 ± 9.5, and 20.7 ± 11.0%, respectively. The lower branching density in the center of the kidney was characteristic for all AOC1-treated preparations at 13.5 d.p.c. (Fig. 6*A*). Notably, degradation of polyamines by AOC1 is expected to increase H_2O_2 production (12, 13). Alteration of ureteric bud branching in response to AOC1 treatment might therefore be due to a critical decrease of polyamines and/or accumulation of cytotoxic H_2O_2. To distinguish between these possibilities, we added AOC1 together with putrescine to the organ cultures. Combined treatment of the tissue specimens with AOC1 (50 milliunits/ml) and putrescine (100 μM) further reduced ($p < 0.5$, paired *t* test) ureter branching at 11.5 (−31.1 ± 25.8%, $n = 6$), 12.5 (−30.0 ± 12.9%, $n = 5$), and 13.5 d.p.c. (−37.3 ± 19.1%, $n = 8$) (Fig. 6*B*). Otherwise, the free radical scavenger vitamin C (200 μM) prevented the inhibition of ureteric bud branching that was caused by AOC1 (Fig. 6*C*). However, combined treatment with AOC1 and vitamin C significantly increased the number of intrarenal branching points at 13.5 d.p.c. (Fig. 6*C*). We therefore assume that impaired ureter growth in response to AOC1 treatment resulted from H_2O_2 cytotoxicity rather than polyamine depletion. Addition of putrescine (100 μM) alone inhibited ureter branching at 13.5 d.p.c. by 15.5 ± 21.2% but had no significant effect during earlier developmental stages (11.5 and 12.5 d.p.c.) (Fig. 7*A*). Aminoguanidine was used to inhibit endogenous AOC1 activity in kidney organ cultures. Incubation with aminoguanidine (1 μM) significantly increased intrarenal ureter branching by 25.7 ± 31.4% at 11.5 d.p.c. but reduced the number of branches by 10.1 ± 15.3% ($p < 0.05$) at 13.5 d.p.c. (Fig. 7*B*). Aminoguanidine had no significant effect on ureteric bud branching at 12.5 d.p.c. (Fig. 7*B*). These findings indicate that branching morphogenesis of the kidney is influenced by polyamines in a developmental stage-specific manner.

DISCUSSION

The mammalian kidney develops through an intricate process of branching morphogenesis, which is initiated by the outgrowth of the ureter from the nephric duct and subsequent invasion into the metanephric mesenchyme (28). During this course, signals emanating from the branching ureteric bud tips induce the mesenchymal cells to aggregate and epithelialize. Epithelial differentiation of the metanephric blastema in turn is a prerequisite for sustained ureter branching and nephron formation (28).

The Wilms tumor protein, WT1, is initially expressed in the condensing mesenchyme of the metanephric kidney and is necessary for the dichotomous growth of the ureteric bud. In the absence of WT1, the cells of the metanephric blastema become apoptotic, the ureteric bud fails to protrude into the surrounding mesenchyme, and epithelialization does not occur (30). *In vitro* organ culture experiments proved a requirement of WT1 not only for the early inductive events but also during the later phases of kidney formation, *i.e.* the differentiation and maturation of nephrons (53). In agreement with a previous investigation (44), we observed a significant reduction in the number of intrarenal ureter branching points upon *Wt1* morpholino treatment at different developmental stages (Fig. 2*D*). These current findings suggest that transcriptional activation of the *Aoc1* gene by WT1 contributes to kidney morphogenesis by regulating putrescine breakdown.

Consistently, administration of external AOC1 significantly reduced ureteric bud branching in murine embryonic kidney explants at 11.5 d.p.c., whereas inhibition of endogenous AOC1

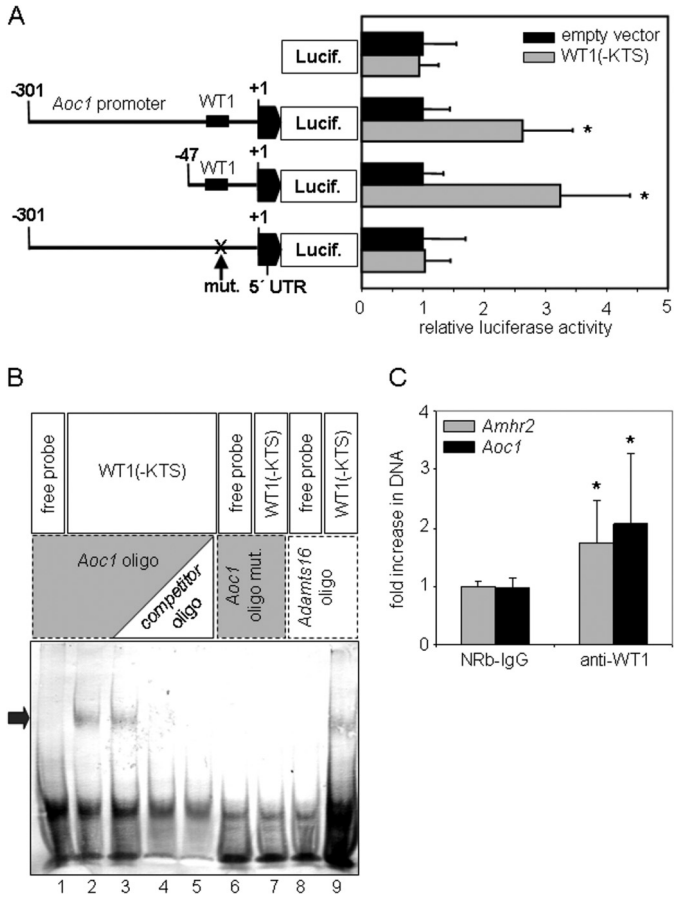

FIGURE 5. **WT1(−KTS) activates the promoter of the *AOC1* gene.** *A*, HEK293 cells were transiently transfected with reporter constructs expressing a firefly luciferase (*Lucif.*) under control of *AOC1* promoter pieces of various lengths. The reporter constructs were co-transfected with either a WT1(−KTS) expression plasmid or empty vector. A *Renilla* luciferase plasmid was utilized for normalization of transfection efficiencies. Data shown are means ± S.E. (*error bars*) ($n = 4$). Statistical significance *versus* transfection with empty expression vector is indicated by an *asterisk* ($p < 0.05$, *t* test). *mut.*, mutation; *B*, binding of WT1(−KTS) to the predicted element (*lane 2 versus lane 1*) in the human *AOC1* promoter was proven by electrophoretic mobility shift assay. Interaction of WT1(−KTS) protein with the *AOC1* promoter oligonucleotide could be competed with excess amounts of unlabeled DNA (*lanes 3–5*) containing the previously identified WT1 binding element of the murine *Adamts16* promoter (43). Mutation of the WT1 consensus motif abrogated WT1(−KTS) binding (*lanes 6* and *7*). Interaction of WT1(−KTS) protein with the *Adamts16* promoter element (43) served as an internal quality control (*lanes 8* and *9*). *C*, ChIP was performed to detect WT1 protein bound to the promoter region of the murine *Aoc1* gene in its native chromosomal configuration. A specific antibody against WT1 was used for immunoprecipitation of chromatin prepared from M15 cells. Incubation with normal rabbit IgG (*NRb-IgG*) served as a negative control. Amplicons encompassing the 5′-flanking region of the *Aoc1* gene were generated by real time PCR. The gene encoding anti-Müllerian hormone receptor 2 (*Amhr2*), a previously identified WT1 target (52), was used as a positive control. Data shown are means ± S.D. (*error bars*). Statistical significances between normal rabbit IgG and anti-WT1 are indicated by an *asterisk* ($p < 0.05$, paired *t* test, $n = 7$).

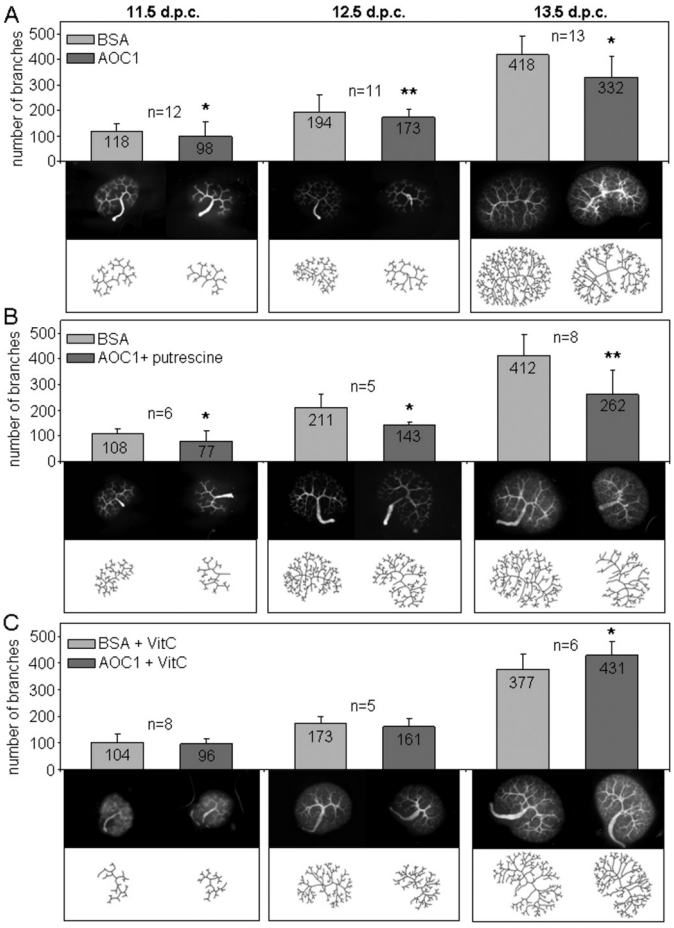

FIGURE 6. **Effect of AOC1, given either alone or in combination with putrescine and vitamin C, respectively, on branching morphogenesis in embryonic kidney explants.** Kidneys were excised from murine embryos at the indicated gestational stages and incubated for 48 h in the presence of AOC1 (50 milliunits/ml) alone (*A*) or together with 100 μM putrescine (*B*) and 200 μM vitamin C (*VitC*) (*C*), respectively. As a control, the contralateral kidney of each embryo was treated with BSA. After 48 h of culture, the ureter was stained with a FITC-conjugated anti-pancytokeratin antibody (dark field images), and a skeleton of the ureteric bud branches was drawn manually (schematic images). Branching of the ureter was analyzed based on the schematic sketches. The absolute numbers of branches are indicated in the *columns*. Data are presented as means ± S.D. (*error bars*). * ($p < 0.05$) and ** ($p < 0.005$) indicate significant differences (paired *t* test).

with aminoguanidine stimulated *in vitro* nephrogenesis at this developmental stage (Figs. 6 and 7). In line with our observation, inhibition of ODC1, the rate-limiting enzyme for polyamine synthesis, has been shown previously to reduce cell proliferation and tubule formation in murine kidney explants at E11.0 (27). The exact mechanism how polyamines influence kidney development is unknown but may involve the regulation of genes acting on the mesenchymal-epithelial balance (27).

Interestingly, aminoguanidine had no significant effect on branching morphogenesis at 12.5 d.p.c. and even inhibited tubule formation at 13.5 d.p.c. (Fig. 7*B*). These findings suggest that the requirement of polyamines for kidney organogenesis is developmental stage-specific. Initially, down-regulation of polyamine breakdown may promote kidney growth presumably by stimulating cell proliferation (27). As kidney formation proceeds, nephron differentiation is favored by a decrease in cell proliferation, and high polyamine levels would thus inhibit branching morphogenesis (53).

It is important to note that aminoguanidine also reduces the activities of other enzymes such as polyamine oxidase, which degrades spermine and spermidine (54), and NO synthase, which is necessary for NO production. However, the K_i values for inhibition of polyamine oxidase (K_i value of 70 μM) and the constitutive (K_i value of 0.83 mM) and inducible (K_i value of 16 μM) NO synthase are far above the K_i value for AOC1 inhibition

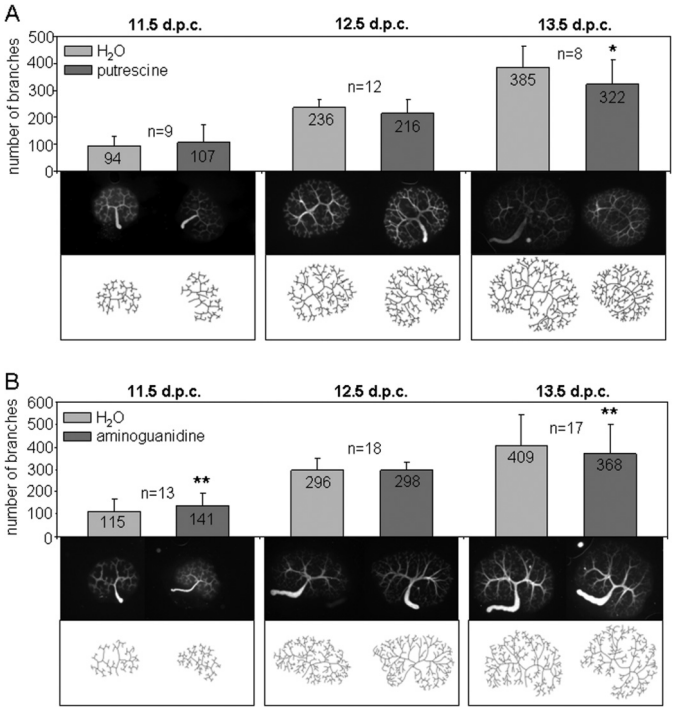

FIGURE 7. **Effect of putrescine and AOC1 inhibition by aminoguanidine on branching morphogenesis in embryonic kidney explants.** Embryonic kidney organ cultures (11.5, 12.5, and 13.5 d.p.c.) were treated for 48 h with 100 μM putrescine (*A*) or 1 μM aminoguanidine to inhibit AOC1 enzyme activity (*B*). The contralateral kidney of each embryo was cultured in the presence of BSA. The preparations were processed and analyzed as described in the legend of Fig. 6. The absolute numbers of branches are given in the *columns*. Data are means ± S.D. (*error bars*). * ($p < 0.05$) and ** ($p < 0.005$) indicate significant differences (paired *t* test).

(K_i value of 50 nM) (54–56). We therefore assume that the treatment of kidney organ cultures with aminoguanidine at a 1 μM concentration was effective primarily through inhibition of AOC1 activity and thus putrescine breakdown.

AOC1 does not only inactivate putrescine but also catalyzes histamine degradation (57). Histamine is produced by the histamine decarboxylase, which is expressed in the developing kidney earliest at 14.5 d.p.c. (58). Changes in histamine metabolism are therefore unlikely to account for the observed effects of AOC1 on ureteric bud branching before this time. It is also noteworthy that degradation of putrescine by AOC1 generates H_2O_2, which might exert toxic effects in embryonic kidney explants. In fact, inhibition of ureteric bud branching in response to external AOC1 was augmented by the simultaneous administration of putrescine (Fig. 6*B*). Furthermore, the free radical scavenger vitamin C prevented the inhibitory effect of AOC1 on ureteric branching at 11.5 and 12.5 d.p.c., and in the presence of vitamin C, AOC1 even increased the number of branching points at 13.5 d.p.c. (Fig. 6*C*). These findings suggest that the detrimental effect of AOC1 was, at least in part, due to the production of cytotoxic H_2O_2 in addition to the depletion of putrescine (59). Hence, our data support the idea that the breakdown of polyamines is beneficial to kidney morphogenesis provided that the concomitant generation of harmful H_2O_2 is compensated by scavenger molecules.

WT1 has previously been reported to regulate the expression of ODC1, the key enzyme for polyamine synthesis, in a rather multifaceted manner. Although overexpression of WT1 in baby hamster kidney cells resulted in a decline of cellular *Odc1* mRNA levels (46), WT1 enhanced *ODC1* promoter activity in SV40-transfected HepG2 cells and repressed activity of the *ODC1* promoter in several other cell lines (29). These findings suggest that the effect of WT1 on *ODC1* expression is complex and cell type-specific. We observed a significant decrease of *Odc1* transcripts in renal organ cultures upon antisense inhibition of *Wt1*, indicating that WT1 stimulates *Odc1* expression in the developing kidney (Fig. 2).

Considering the antagonistic functions of ODC1 and AOC1 in polyamine metabolism, it seems puzzling at first glance that WT1 up-regulates both genes in embryonic kidneys (Fig. 2). In this regard, one has to keep in mind that distinct cell populations in embryonic kidneys may exhibit a specific and variable demand for polyamines during successive phases of differentiation. High levels of *Odc1* mRNA were detected in ureteric bud cells, suggesting that ureter branching requires active polyamine synthesis (27). Importantly, polyamines and their diamine precursor, putrescine, are secreted molecules that can be taken up by neighboring cells through membrane transporters (60). Thus, a rise of polyamines in the metanephric mesenchyme due to secretion from the invading ureteric bud tips might be detrimental to nephron differentiation. In agreement with this possibility, incubation of murine embryonic kidney explants in the presence of putrescine significantly reduced ureter branching at 13.5 d.p.c. (Fig. 7*A*). Hence, stimulation of *Aoc1* expression by WT1 may fulfill the purpose of fine-tuning polyamine levels in a spatial and temporal manner. This idea is supported by the co-expression of WT1 and AOC1 proteins in developing glomeruli of embryonic kidneys (Fig. 1*d*).

Stimulation of *Aoc1* expression by WT1 may also become important for the development and function of the gonads. The mammalian gonads are formed by tissue derived from the intermediate mesoderm on either side of the embryonic midline axis (61). Development of the bipotential gonadal ridge occurs in a non-sex-specific manner in XX and XY individuals and is completed by 12 d.p.c. in rats and mice (62). WT1 acts on multiple steps during gonad development. Thus, gonadal ridge formation in *Wt1*-deficient mice is initiated in both males and females but then degenerates due to apoptosis, leading to gonadal agenesis (30). Polyamines are essential to male and female reproductive processes. In male reproduction, polyamines correlate with stages of spermatogenesis and regulate sperm cell motility (63). In female mammals, polyamines are involved in ovarian follicle development and ovulation (63). Recent findings have demonstrated that these processes in the male and female reproductive system also require WT1 (64, 65). Thus, it appears plausible that the effects of WT1 in the gonads of both sexes are mediated to some extent by the control of polyamine homeostasis.

In summary, normal formation of the genitourinary system requires a precise adjustment of polyamines during different developmental stages. Previous studies have shown that this can be accomplished by a tight regulation of ODC1 activity (66). Our data suggest that WT1-dependent stimulation of *Aoc1* gene expression contributes to the harmonization of polyamine levels in embryonic kidneys with the actual needs. Down-regulation of AOC1 due to inactivation of *Wt1* is expected to disturb

the delicate balance of growth-promoting and prodifferentiating signals, thereby favoring a proliferative phenotype. Intriguingly, a significant increase in free polyamines has been reported in the peripheral blood of Wilms tumor patients (67). In light of this observation and our current findings, it might be rewarding to investigate the role of AOC1 expression and polyamine metabolism in human Wilms tumors in more detail.

Acknowledgments—We thank Ulrike Neumann and Sabine Schröter for expert technical assistance.

REFERENCES

1. Kusano, T., Berberich, T., Tateda, C., and Takahashi, Y. (2008) Polyamines: essential factors for growth and survival. *Planta* **228,** 367–381
2. Feuerstein, B. G., Williams, L. D., Basu, H. S., and Marton, L. J. (1991) Implications and concepts of polyamine-nucleic acid interactions. *J. Cell. Biochem.* **46,** 37–47
3. Matthews, H. R. (1993) Polyamines, chromatin structure and transcription. *BioEssays* **15,** 561–566
4. Gerner, E. W., and Meyskens, F. L., Jr. (2004) Polyamines and cancer: old molecules, new understanding. *Nat. Rev. Cancer* **4,** 781–792
5. Moinard, C., Cynober, L., and de Bandt, J. P. (2005) Polyamines: metabolism and implications in human diseases. *Clin. Nutr.* **24,** 184–197
6. Kim, G. H., Komotar, R. J., McCullough-Hicks, M. E., Otten, M. L., Starke, R. M., Kellner, C. P., Garrett, M. C., Merkow, M. B., Rynkowski, M., Dash, K. A., and Connolly, S. (2009) The role of polyamine metabolism in neuronal injury following cerebral ischemia. *Can. J. Neurol. Sci.* **36,** 14–19
7. Soda, K. (2011) The mechanisms by which polyamines accelerate tumor spread. *J. Exp. Clin. Cancer Res.* **30,** 95
8. Zahedi, K., and Soleimani, M. (2011) Spermidine/spermine-N^1-acetyltransferase in kidney ischemia reperfusion injury. *Methods Mol. Biol.* **720,** 379–394
9. Tantini, B., Fiumana, E., Cetrullo, S., Pignatti, C., Bonavita, F., Shantz, L. M., Giordano, E., Muscari, C., Flamigni, F., Guarnieri, C., Stefanelli, C., and Caldarera, C. M. (2006) Involvement of polyamines in apoptosis of cardiac myoblasts in a model of stimulated ischemia. *J. Mol. Cell. Cardiol.* **40,** 775–782
10. Tabor, C. W., and Tabor, H. (1984) Polyamines. *Annu. Rev. Biochem.* **53,** 749–790
11. Pegg, A. E. (1986) Recent advances in the biochemistry of polyamines in eukaryotes. *Biochem. J.* **234,** 249–262
12. Seiler, N. (2004) Catabolism of polyamines. *Amino Acids* **26,** 217–233
13. Pegg, A. E. (2008) Spermidine/spermine-N^1-acetyltransferase: a key metabolic regulator. *Am. J. Physiol. Endocrinol. Metab.* **294,** E995–E1010
14. Barbry, P., Champe, M., Chassande, O., Munemitsu, S., Champigny, G., Lingueglia, E., Maes, P., Frelin, C., Tartar, A., Ullrich, A., and Lazdunski, M. (1990) Human kidney amiloride-binding protein: cDNA structure and functional expression. *Proc. Natl. Acad. Sci. U.S.A.* **87,** 7347–7351
15. Schwelberger, H. G., and Bodner, E. (1997) Purification and characterization of diamine oxidase from porcine kidney and intestine. *Biochim. Biophys. Acta* **1340,** 152–164
16. Chassande, O., Renard, S., Barbry, P., and Lazdunski, M. (1994) The human gene for diamine oxidase, an amiloride binding protein. Molecular cloning, sequencing, and characterization of the promoter. *J. Biol. Chem.* **269,** 14484–14489
17. Novotny, W. F., Chassande, O., Baker, M., Lazdunski, M., and Barbry, P. (1994) Diamine oxidase is the amiloride-binding protein and is inhibited by amiloride analogues. *J. Biol. Chem.* **269,** 9921–9925
18. Biegański, T., Osińska, Z., and Maśliński, C. (1982) Inhibition of plant and mammalian diamine oxidases by hydrazine and guanidine compounds. *Int. J. Biochem.* **14,** 949–953
19. Sebela, M., Tylichová, M., and Pec, P. (2007) Inhibition of diamine oxidases and polyamine oxidases by diamine-based compounds. *J. Neural Transm.* **114,** 793–798
20. Schwelberger, H. G., and Bodner, E. (1998) Identity of the diamine oxidase proteins in porcine kidney and intestine. *Inflamm. Res.* **47,** Suppl. 1, S58–S59
21. Klocker, J., Mätzler, S. A., Huetz, G. N., Drasche, A., Kolbitsch, C., and Schwelberger, H. G. (2005) Expression of histamine degrading enzymes in porcine tissues. *Inflamm. Res.* **54,** Suppl. 1, S54–S57
22. Morel, F., Surla, A., and Vignais, P. V. (1992) Purification of human placenta diamine oxidase. *Biochem. Biophys. Res. Commun.* **187,** 178–186
23. Biegański, T., Kusche, J., Lorenz, W., Hesterberg, R., Stahlknecht, C. D., and Feussner, K. D. (1983) Distribution and properties of human intestinal diamine oxidase and its relevance for the histamine catabolism. *Biochim. Biophys. Acta* **756,** 196–203
24. Raithel, M., Küfner, M., Ulrich, P., and Hahn, E. G. (1999) The involvement of the histamine degradation pathway by diamine oxidase in manifest gastrointestinal allergies. *Inflamm. Res.* **48**, Suppl. 1, S75–S76
25. Elmore, B. O., Bollinger, J. A., and Dooley, D. M. (2002) Human kidney diamine oxidase: heterologous expression, purification, and characterization. *J. Biol. Inorg. Chem.* **7,** 565–579
26. Liang, X. H., Zhao, Z. A., Deng, W. B., Tian, Z., Lei, W., Xu, X., Zhang, X. H., Su, R. W., and Yang, Z. M. (2010) Estrogen regulates amiloride-binding protein 1 through CCAAT/enhancer-binding protein-β in mouse uterus during embryo implantation and decidualization. *Endocrinology* **151,** 5007–5016
27. Loikkanen, I., Lin, Y., Railo, A., Pajunen, A., and Vainio, S. (2005) Polyamines are involved in murine kidney development controlling expression of c-ret, E-cadherin, and Pax2/8 genes. *Differentiation* **73,** 303–312
28. Michos, O. (2009) Kidney development: from ureteric bud formation to branching morphogenesis. *Curr. Opin. Genet. Dev.* **19,** 484–490
29. Moshier, J. A., Skunca, M., Wu, W., Boppana, S. M., Rauscher, F. J., 3rd, and Dosescu, J. (1996) Regulation of ornithine decarboxylase gene expression by the Wilms' tumor suppressor WT1. *Nucleic Acids Res.* **24,** 1149–1157
30. Kreidberg, J. A., Sariola, H., Loring, J. M., Maeda, M., Pelletier, J., Housman, D., and Jaenisch, R. (1993) WT-1 is required for early kidney development. *Cell* **74,** 679–691
31. Moore, A. W., McInnes, L., Kreidberg, J., Hastie, N. D., and Schedl, A. (1999) YAC complementation shows a requirement for Wt1 in the development of epicardium, adrenal gland and throughout nephrogenesis. *Development* **126,** 1845–1857
32. Herzer, U., Crocoll, A., Barton, D., Howells, N., and Englert, C. (1999) The Wilms tumor suppressor gene Wt1 is required for development of the spleen. *Curr. Biol.* **9,** 837–840
33. Wagner, K. D., Wagner, N., Vidal, V. P., Schley, G., Wilhelm, D., Schedl, A., Englert, C., and Scholz, H. (2002) The Wilms' tumor gene *Wt1* is required for retinal development. *EMBO J.* **21,** 1398–1405
34. Wagner, N., Wagner, K. D., Hammes, A., Kirschner, K. M., Vidal, V. P., Schedl, A., and Scholz, H. (2005) A splice variant of the Wilms' tumour suppressor Wt1 is required for normal development of the olfactory system. *Development* **132,** 1327–1336
35. Wagner, N., Wagner, K. D., Theres, H., Englert, C., Schedl, A., and Scholz, H. (2005) Coronary vessel development requires activation of the TrkB neurotrophin receptor by the Wilms' tumor transcription factor Wt1. *Genes Dev.* **19,** 2631–2642
36. Clapcote, S. J., and Roder, J. C. (2005) Simplex PCR assay for sex determination in mice. *BioTechniques* **38,** 702
37. Englert, C., Hou, X., Maheswaran, S., Bennett, P., Ngwu, C., Re, G. G., Garvin, A. J., Rosner, M. R., and Haber, D. A. (1995) WT1 suppresses synthesis of the epidermal growth factor receptor and induces apoptosis. *EMBO J.* **14,** 4662–4675
38. Larsson, S. H., Charlieu, J. P., Miyagawa, K., Engelkamp, D., Rassoulzadegan, M., Ross, A., Cuzin, F., van Heyningen, V., and Hastie, N. D. (1995) Subnuclear localization of WT1 in splicing or transcription factor domains is regulated by alternative splicing. *Cell* **81,** 391–401
39. Sciesielski, L. K., Kirschner, K. M., Scholz, H., and Persson, A. B. (2010) Wilms' tumor protein Wt1 regulates the Interleukin-10 (IL-10) gene. *FEBS Lett.* **584,** 4665–4671
40. Dame, C., Kirschner, K. M., Bartz, K. V., Wallach, T., Hussels, C. S., and Scholz, H. (2006) Wilms tumor suppressor, Wt1, is a transcriptional activator of the erythropoietin gene. *Blood* **107,** 4282–4290

41. Kirschner, K. M., Hagen, P., Hussels, C. S., Ballmaier, M., Scholz, H., and Dame, C. (2008) The Wilms' tumor suppressor Wt1 activates transcription of the erythropoietin receptor in hematopoietic progenitor cells. *FASEB J.* **22,** 2690–2701
42. Wagner, K. D., Wagner, N., Sukhatme, V. P., and Scholz, H. (2001) Activation of vitamin D receptor by the Wilms' tumor gene product mediates apoptosis of renal cells. *J. Am. Soc. Nephrol.* **12,** 1188–1196
43. Jacobi, C. L., Rudigier, L. J., Scholz, H., and Kirschner, K. M. (2013) Transcriptional regulation by the Wilms tumor protein, Wt1, suggests a role of the metalloproteinase Adamts16 in murine genitourinary development. *J. Biol. Chem.* **288,** 18811–18824
44. Hartwig, S., Ho, J., Pandey, P., Macisaac, K., Taglienti, M., Xiang, M., Alterovitz, G., Ramoni, M., Fraenkel, E., and Kreidberg, J. A. (2010) Genomic characterization of Wilms' tumor suppressor 1 targets in nephron progenitor cells during kidney development. *Development* **137,** 1189–1203
45. Martens, L. K., Kirschner, K. M., Warnecke, C., and Scholz, H. (2007) Hypoxia-inducible factor-1 (HIF-1) is a transcriptional activator of the TrkB neurotrophin receptor gene. *J. Biol. Chem.* **282,** 14379–14388
46. Li, R. S., Law, G. L., Seifert, R. A., Romaniuk, P. J., and Morris, D. R. (1999) Ornithine decarboxylase is a transcriptional target of tumor suppressor WT1. *Exp. Cell Res.* **247,** 257–266
47. Haber, D. A., Sohn, R. L., Buckler, A. J., Pelletier, J., Call, K. M., and Housman, D. E. (1991) Alternative splicing and genomic structure of the Wilms tumor gene WT1. *Proc. Natl. Acad. Sci. U.S.A.* **88,** 9618–9622
48. Madden, S. L., Cook, D. M., Morris, J. F., Gashler, A., Sukhatme, V. P., and Rauscher, F. J., 3rd (1991) Transcriptional repression mediated by the WT1 Wilms tumor gene product. *Science* **253,** 1550–1553
49. Hamilton, T. B., Barilla, K. C., and Romaniuk, P. J. (1995) High affinity binding sites for the Wilms' tumour suppressor protein WT1. *Nucleic Acids Res.* **23,** 277–284
50. Laity, J. H., Dyson, H. J., and Wright, P. E. (2000) Molecular basis for modulation of biological function by alternate splicing of the Wilms' tumor suppressor protein. *Proc. Natl. Acad. Sci. U.S.A.* **97,** 11932–11935
51. Bor, Y. C., Swartz, J., Morrison, A., Rekosh, D., Ladomery, M., and Hammarskjöld, M. L. (2006) The Wilms' tumor 1 (WT1) gene (+KTS isoform) functions with a CTE to enhance translation from an unspliced RNA with a retained intron. *Genes Dev.* **20,** 1597–1608
52. Klattig, J., Sierig, R., Kruspe, D., Besenbeck, B., and Englert, C. (2007) Wilms' tumor protein Wt1 is an activator of the anti-Müllerian hormone receptor gene Amhr2. *Mol. Cell. Biol.* **27,** 4355–4364
53. Davies, J. A., Ladomery, M., Hohenstein, P., Michael, L., Shafe, A., Spraggon, L., and Hastie, N. (2004) Development of an siRNA-based method for repressing specific genes in renal organ culture and its use to show that the Wt1 tumour suppressor is required for nephron differentiation. *Hum. Mol. Genet.* **13,** 235–246
54. Gahl, W. A., and Pitot, H. C. (1982) Polyamine degradation in foetal and adult bovine serum. *Biochem. J.* **202,** 603–611
55. Beaven, M. A., and Roderick, N. B. (1980) Impromidine, a potent inhibitor of histamine methyltransferase (HMT) and diamine oxidase (DAO). *Biochem. Pharmacol.* **29,** 2897–2900
56. Wolff, D. J., and Lubeskie, A. (1995) Aminoguanidine is an isoform-selective, mechanism-based inactivator of nitric oxide synthase. *Arch. Biochem. Biophys.* **316,** 290–301
57. Mizuguchi, H., Imamura, I., Takemura, M., and Fukui, H. (1994) Purification and characterization of diamine oxidase (histaminase) from rat small intestine. *J. Biochem.* **116,** 631–635
58. Karlstedt, K., Nissinen, M., Michelsen, K. A., and Panula, P. (2001) Multiple sites of L-histidine decarboxylase expression in mouse suggest novel developmental functions for histamine. *Dev. Dyn.* **221,** 81–91
59. Sharmin, S., Sakata, K., Kashiwagi, K., Ueda, S., Iwasaki, S., Shirahata, A., and Igarashi, K. (2001) Polyamine cytotoxicity in the presence of bovine serum amine oxidase. *Biochem. Biophys. Res. Commun.* **282,** 228–235
60. Abdulhussein, A. A., and Wallace, H. M. (2014) Polyamines and membrane transporters. *Amino Acids* **46,** 655–660
61. Quinn, A., and Koopman, P. (2012) The molecular genetics of sex determination and sex reversal in mammals. *Semin. Reprod. Med.* **30,** 351–363
62. Swain, A., and Lovell-Badge, R. (1999) Mammalian sex determination: a molecular drama. *Genes Dev.* **13,** 755–767
63. Lefèvre, P. L., Palin, M. F., and Murphy, B. D. (2011) Polyamines on the reproductive landscape. *Endocr. Rev.* **32,** 694–712
64. Zheng, Q. S., Wang, X. N., Wen, Q., Zhang, Y., Chen, S. R., Zhang, J., Li, X. X., Sha, R. N., Hu, Z. Y., Gao, F., and Liu, Y. X. (2014) Wt1 deficiency causes undifferentiated spermatogonia accumulation and meiotic progression disruption in neonatal mice. *Reproduction* **147,** 45–52
65. Gao, F., Zhang, J., Wang, X., Yang, J., Chen, D., Huff, V., and Liu, Y. X. (2014) Wt1 functions in ovarian follicle development by regulating granulosa cell differentiation. *Hum. Mol. Genet.* **23,** 333–341
66. Shantz, L. M., and Levin, V. A. (2007) Regulation of ornithine decarboxylase during oncogenic transformation: mechanisms and therapeutic potential. *Amino Acids* **33,** 213–223
67. Balitskaia, O. V., Berdinskikh, N. K., and Kononenko, N. G. (1992) The possibilities of using the free polyamines of the peripheral blood as biochemical tumor markers in nephroblastoma in children. *Vopr. Onkol.* **38,** 674–682